

## Role of the similar molecular weight dyes on the adsorption by activated carbon

Monika Chaudhary<sup>a</sup>, Suhas<sup>a,\*</sup>, Randhir Singh<sup>a</sup>, Murat Yilmaz<sup>b</sup>, Shubham Chaudhary<sup>a</sup>, Sarita Kushwaha<sup>a</sup>

<sup>a</sup>Department of Chemistry, Gurukula Kangri (Deemed to be University), Haridwar – 249404, India, emails: suhasnatyan@yahoo.com/suhas@gkv.ac.in (Suhas), monikachoudry@gmail.com (M. Chaudhary), randhirchem@yahoo.com (R. Singh), shubhamchaudhary89@yahoo.com (S. Chaudhary), saritakushwaha31@gmail.com (S. Kushwaha)

<sup>b</sup>Osmaniye Korkut Ata University, Faculty of Engineering, Department of Chemical Engineering, 80000, Osmaniye, Turkey, email: muratyilmaz@osmaniye.edu.tr

Received 20 May 2021; Accepted 20 October 2021

### ABSTRACT

In the current study, the effect on the adsorption of dyes (Basic red 2, Basic blue 3 and Ethyl orange) having almost similar molecular weight but belonging to different classes and functional groups on air activated carbon prepared from demineralised kraft lignin (DKLAAC) was investigated. The experimental and theoretical adsorption values for the dyes on DKLAAC were found to be 0.599, 0.550 and 0.395 mmol g<sup>-1</sup> and 0.569, 0.520 and 0.387 mmol g<sup>-1</sup> for Basic red 2, Basic blue 3 and Ethyl orange, respectively. Basic red 2 showed maximum adsorption (0.599 mmol g<sup>-1</sup>) on DKLAAC owing to more hydrophobicity and resonance in its structure. Contrarily, Ethyl orange showed minimum adsorption due to the hydrophilicity and less number of benzene rings. The presence of acid/basic site concentration of DKLAAC also affects the adsorption process. The obtained experimental data fitted best to the pseudo-second-order kinetic model. Thermodynamic parameters analysed confirms the feasibility, spontaneity and endothermic nature of the adsorption process.

*Keywords:* Adsorption; Dyes; Kraft lignin; Activated carbon

### 1. Introduction

Dyes constitute one of the most polluting agents in water systems due to their stability and poor biodegradability. Various techniques [1–15] have been utilised for the removal of pollutants including dyes. However, among these techniques adsorption process is found to be a versatile methodology for the removal of various types of dyes [15]. Several parameters viz. adsorbate concentration, surface area, solution temperature, pore size etc. are found to affect the adsorption phenomenon in the case of the dyes. Among these what role a class or functional group of a dye can play especially in the case of similar molecular weight is discussed less in the literature. Therefore, the current study

is focused on the adsorption behavior of dyes having similar molecular weight but of different class and functional groups.

Dyes as well-known can be classified viz. acid, basic, direct, reactive, vat and disperse dyes [15]. Among these acid and basic dyes are important especially for colouring industries because of their high stability to light and temperature, appreciable solubility in water, favourable characteristics of bright color and even cost-effectiveness in the synthesis [16]. The main chemical classes of acid dyes are azo, triphenylmethane, anthraquinone, xanthene, nitro and nitroso, whereas, the principal chemical classes of basic dyes are oxazine, triarylmethane, diazahemicyanine, cyanine, hemicyanine, thiazine, azine and acridine [15].

\* Corresponding author.

For this study, Basic red 2 from azine class, Basic blue 3 from oxazine class and Ethyl orange from the azo class were chosen. It is interesting to note that all these dyes have molecular weight of nearly 355. Basic red 2 also known as safranin O has a historical interest since the first synthetic dyes mauveine belongs to this class and is closely related to it [17]. Basic blue 3, belongs to a small group of little significance in textile applications [18]. Also, new uses have been found in biomedical applications because of fluorescence, as laser dyes and dopants in organic light-emitting diodes [19]. Commonly these both dyes are used for colouring of the paper, polyacrylonitrile, modified nylons, modified polyesters, polyethylene terephthalate, silk, wool, and tannin-mordanted cotton [15]. Ethyl orange on another side consists of an azo group with nitrogen nitrogen double bonds ( $-N=N-$ ). Acid azo dyes are generally used for dyeing and printing wool, polyamide, silk, and basic-modified acrylics and dyeing leather, fur, paper, and food [20].

Keeping this in view herein the adsorptive behavior of dye molecules belonging to different classes but the nearly same molecular weight on activated carbon developed from demineralised kraft lignin in the air (DKLAAC) at 950°C will be studied. The objective of the present work is also to investigate the adsorption potential of DKLAAC for the removal of acid as well as basic dyes having an almost the same molecular weight from aqueous solutions. To understand the adsorption properties, the adsorption isotherms and kinetics of the selected dyes onto DKLAAC were measured. Besides these, the spontaneity, as well as thermodynamic feasibility of the adsorption processes with respect to thermodynamic parameters is discussed too. In order to assess the potential of the adsorbents with regard to dye removal, the performance has been evaluated with respect to a commercial activated carbon (CAC) at 25°C. The results of investigations are expected to reveal the effect of class

and functional groups on their adsorption at DKLAAC. Furthermore, the effect of different parameters such as contact time, initial dye concentration and temperature on the adsorption is also analysed.

## 2. Materials and methods

Ethyl orange and Basic blue 3 were procured from Sigma-Aldrich, whereas, Basic red 2 was procured from SRL (India). The structures and selected properties of dyes are given in Table 1. All other chemicals used were of analytical grade. Standard commercial activated carbon (CAC) was procured from Rankem (India). The raw kraft lignin sample was procured from Lignotech Iberica (Spain), and was converted into demineralised kraft lignin (precursor for DKLAAC) by a demineralisation process as discussed elsewhere [21]. For the preparation of DKLAAC, 5 g of demineralised kraft lignin (DKL) was physically activated in a conventional muffle furnace at 950°C at a heating rate of 8°C min<sup>-1</sup> (30 min) in the presence of oxidising atmosphere (air) [21].

The DKLAAC and CAC were characterised with the help of FE-SEM (Tescan Mira 3) and FTIR (Perkin Elmer model Paragon 1000PC spectrophotometer and Perkin Elmer spectrum two). The textural properties of the samples were studied with the help of nitrogen adsorption at 77 K (Quantachrome Quadrasorb 3SI and Micromeritics ASAP 2010) [21]. Acid/basic sites and pzc of the activated carbons (DKLAAC and CAC) were determined by titration method using a procedure discussed elsewhere [22]. The physicochemical properties of DKLAAC and CAC are briefly summarised in Table 2 and discussed in detail elsewhere [21,23]. Double distilled water was used throughout for the preparation of solutions.

Adsorption studies using batch technique being simple and easy to operate were carried out to assess the adsorption

Table 1  
Characteristic properties of similar molecular weight dyes

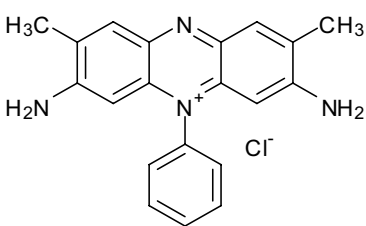
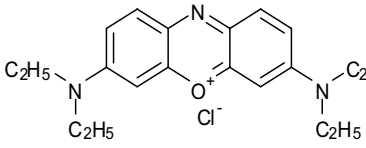
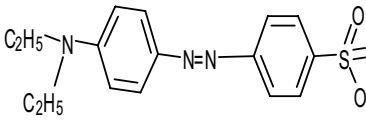
| Name of dye  | Molecular structure   | $\lambda_{\max}$ (nm) | Mol. weight | Chemical class | Molecular formula   |
|--------------|---|-----------------------|-------------|----------------|---|
| Basic red 2  |  | 520                   | 350.85      | Azine          | C <sub>20</sub> H <sub>19</sub> ClN <sub>4</sub>                  |
| Basic blue 3 |  | 655                   | 359.89      | Oxazine        | C <sub>20</sub> H <sub>26</sub> ClN <sub>3</sub> O                |
| Ethyl orange |  | 475                   | 355.39      | Azo            | C <sub>16</sub> H <sub>18</sub> N <sub>3</sub> NaO <sub>3</sub> S |

Table 2  
Physicochemical properties of activated carbons

| DKLAAC   |  | CAC  |
|--|--|--|
| (i) Field-emission scanning electron microscopy* <sup>1</sup>        | Surface of DKLAAC clearly shows porosity and cavities  | Surface of CAC shows porosity and ash  |
| (ii) Fourier-transform infrared spectroscopic analysis* <sup>1</sup> | 1,117 (C–O–C, ether)<br>1,389 cm <sup>-1</sup> (C–H bend in CH <sub>3</sub> )<br>1,559 cm <sup>-1</sup> (C=C aromatic rings)<br>3,400 cm <sup>-1</sup> (hydroxyl groups) | 1,120 (C–O–C, ether)<br>1,398 cm <sup>-1</sup> (C–H bend in CH <sub>3</sub> )<br>1,582 cm <sup>-1</sup> (C=C aromatic rings)<br>3,415 cm <sup>-1</sup> (hydroxyl groups) |
| (iii) Textural analysis* <sup>1</sup>                                |  |  |
| Total surface area (m <sup>2</sup> g <sup>-1</sup> )                 | 1,305  | 770  |
| Mean pore width (nm)   | 1.12   | 2.66   |
| Total pore volume (cm <sup>3</sup> g <sup>-1</sup> )                 | 0.472  | 0.512  |
| (iv) Mass titration  |  |  |
| pH <sub>pzc</sub>  | 7.5  | 7.6  |
| (v) Acid/basic sites concentration                                   |  |  |
| Acid sites   | 0.560 mmol g <sup>-1</sup>   | 0.579 mmol g <sup>-1</sup>   |
| Basic sites  | 0.365 mmol g <sup>-1</sup>   | 0.360 mmol g <sup>-1</sup>   |

behavior of dyes. For this, a fixed amount of DKLAAC (0.01 g) was added to 10 mL of dyes solution of varying concentrations taken in stopper glass tubes and were placed in thermostat cum shaking assembly. The solutions were stirred continuously at constant temperatures for 300 min for acid and basic dyes, to achieve equilibration. The concentration of the dye in the solution after complete equilibrium adsorption was determined spectrophotometrically at  $\lambda_{\max}$  of the adsorbate. The experiments were repeated a number of times and average values are reported.

### 3. Results and discussion

#### 3.1. Effect of contact time and initial concentration

The contact time is an important parameter for the analysis of equilibrium time for the maximum adsorption of dyes. To study this, the adsorptive removal of Basic red 2, Basic blue 3 and Ethyl orange at the fixed concentration on DKLAAC was investigated as a function of contact time and the results are presented in Fig. 1. Results show that the uptake of these dyes was fast initially due to the availability of accessible pores/active sites and free functional groups attached to the surface. Additionally, less steric hindrance was experienced by the adsorbate molecules. With the increase in contact time, the process slows down which was assigned to the less availability of adsorption sites on DKLAAC and increase in the steric hindrance of dye molecules [24]. Maximum removal of the dyes takes place in <40 min and for all dyes, it takes 240 min to reach the equilibrium. Thus for all equilibrium adsorption studies, the contact time was kept at 300 min.

The effect of initial concentration on the adsorption performance was also investigated at varying concentrations

( $4 \times 10^{-4}$  and  $5 \times 10^{-4}$  M). The results are shown in Fig. 2 for Basic red 2 and similar plots were also observed for Basic blue 3 and Ethyl orange (figures not provided). The plot shows that the amount of dye adsorbed per unit mass of DKLAAC increased on increasing the initial dye concentration [25].

Therefore, an increase in initial dye concentration enhances the adsorption of dyes on DKLAAC which is due to the increase in the driving force of concentration gradient on increasing the initial concentration of the adsorbate. The initial concentration provides the necessary driving force to overcome the resistance to the mass transfer of the adsorbate between the aqueous and solid phases [26,27].

#### 3.2. Adsorption isotherms

To investigate the interactive behavior between the adsorbate and adsorbent and the maximum adsorptive capacity for the removal of the dyes having almost same molecular weight but differing in class and functional groups, adsorption isotherms were obtained as a function of equilibrium concentration and shown in Fig. 3. The experimental adsorption values (Table 3) of the dyes on DKLAAC at 25°C were found to be 0.599, 0.550 and 0.395 mmol g<sup>-1</sup> for Basic red 2, Basic blue 3 and Ethyl orange, respectively, which are in the order: Basic red 2 > Basic blue 3 > Ethyl orange. DKLAAC possesses

A comparison was also made with raw demineralised kraft lignin (precursor) and a commercial activated carbon in order to test the performance of DKLAAC and the obtained isotherms are shown in Figs. 4–6. Similar to DKLAAC, the adsorption of dyes on commercial activated carbon was also found to be in order Basic red 2 > Basic blue 3 > Ethyl orange. However, the amount of dyes adsorbed

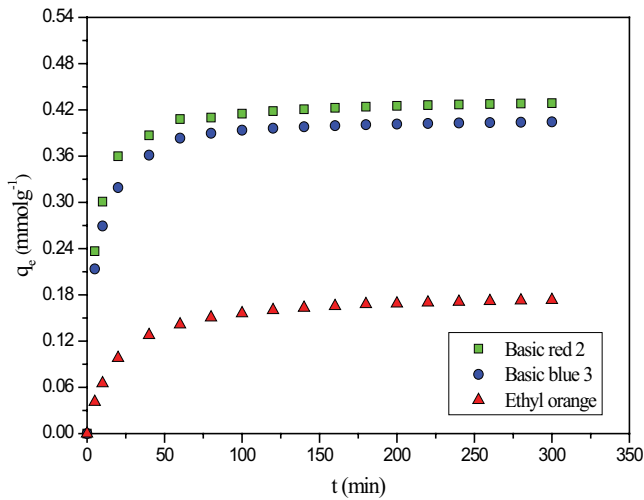


Fig. 1. Effect of contact time for the removal of Basic red 2, Basic blue 3 and Ethyl orange on DKLAAC ( $C_i$ :  $5 \times 10^{-4}$  M;  $T$ :  $25^\circ\text{C}$ ).

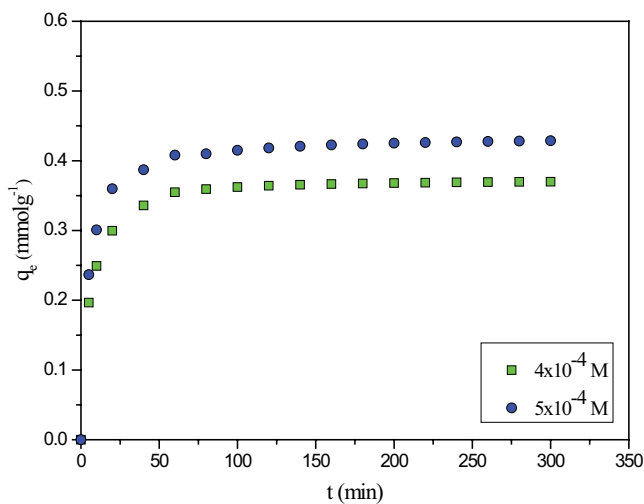


Fig. 2. Effect of initial concentration for the removal of Basic red 2 on DKLAAC at different initial concentrations ( $T$ :  $25^\circ\text{C}$ ).

0.455, 0.411 and 0.341  $\text{mmol g}^{-1}$  for Basic red 2, Basic blue 3 and Ethyl orange, respectively on CAC was found to be comparatively lower than DKLAAC owing to its lower surface area ( $770 \text{ m}^2 \text{ g}^{-1}$ ) and already discussed elsewhere [21]. In the case of demineralised kraft lignin (DKL), interestingly the adsorption of Basic red 2, Basic blue 3 was found to be more compared to acid dyes owing to its negatively charged surface which attracts positively charged dyes (basic dyes) more easily. The amount of adsorption of Basic red 2 and Basic blue 3 by DKL was found  $6.42 \times 10^{-3}$  and  $6.15 \times 10^{-3} \text{ mmol g}^{-1}$ , respectively but it was found to be negligible in the case of Ethyl orange (values and graphs are not provided) due to very low surface area and the negatively charged surface.

It is worth mentioning that a few studies have been reported on the adsorption of Basic blue 3, Basic red 2 and Ethyl orange on various adsorbents. The adsorption

Table 3  
Experimental adsorption values, Langmuir and Freundlich isotherm parameters for the removal of similar molecular weight acid/basic dyes on DKLAAC

| Dyes         | Temperature ( $^\circ\text{C}$ ) | Experimental                            |   | Langmuir isotherm parameters              |   |                              | Freundlich isotherm parameters |                                |      |       |
|--------------|----------------------------------|---|---|---|---|------------------------------|--------------------------------|--------------------------------|------|-------|
|              |                                  | $q_{\text{exp}}$ ( $\text{mg g}^{-1}$ ) | $q_{\text{exp}}$ ( $\text{mmol g}^{-1}$ ) | $q_{\text{max}}$ ( $\text{mmol g}^{-1}$ ) | $q_{\text{max}}$ ( $\text{mg g}^{-1}$ ) | $b$ ( $\text{L mmol}^{-1}$ ) | $R^2$                          | $K_f$ ( $\text{mmol g}^{-1}$ ) | $n$  | $R^2$ |
| Basic red 2  | 25                               | 210                                     | 0.599                                     | 0.569                                     | 199                                     | $7.14 \times 10^4$           | 0.998                          | 22.2                           | 2.47 | 0.915 |
|              | 35                               | 214                                     | 0.611                                     | 0.602                                     | 211                                     | $7.09 \times 10^4$           | 0.999                          | 26.9                           | 2.39 | 0.907 |
|              | 45                               | 218                                     | 0.620                                     | 0.606                                     | 213                                     | $7.90 \times 10^4$           | 0.996                          | 32.1                           | 2.33 | 0.916 |
| Basic blue 3 | 25                               | 197                                     | 0.550                                     | 0.520                                     | 186                                     | $6.93 \times 10^4$           | 0.995                          | 11.7                           | 2.79 | 0.896 |
|              | 35                               | 205                                     | 0.570                                     | 0.564                                     | 203                                     | $7.04 \times 10^4$           | 0.997                          | 19.0                           | 2.54 | 0.915 |
|              | 45                               | 213                                     | 0.589                                     | 0.569                                     | 205                                     | $7.46 \times 10^4$           | 0.996                          | 33.6                           | 2.27 | 0.934 |
| Ethyl orange | 25                               | 140                                     | 0.395                                     | 0.387                                     | 137                                     | $3.89 \times 10^4$           | 0.996                          | 6.7                            | 2.87 | 0.926 |
|              | 35                               | 151                                     | 0.425                                     | 0.403                                     | 143                                     | $4.07 \times 10^4$           | 0.994                          | 7.2                            | 2.86 | 0.921 |
|              | 45                               | 158                                     | 0.443                                     | 0.427                                     | 152                                     | $4.12 \times 10^4$           | 0.995                          | 8.4                            | 2.78 | 0.919 |

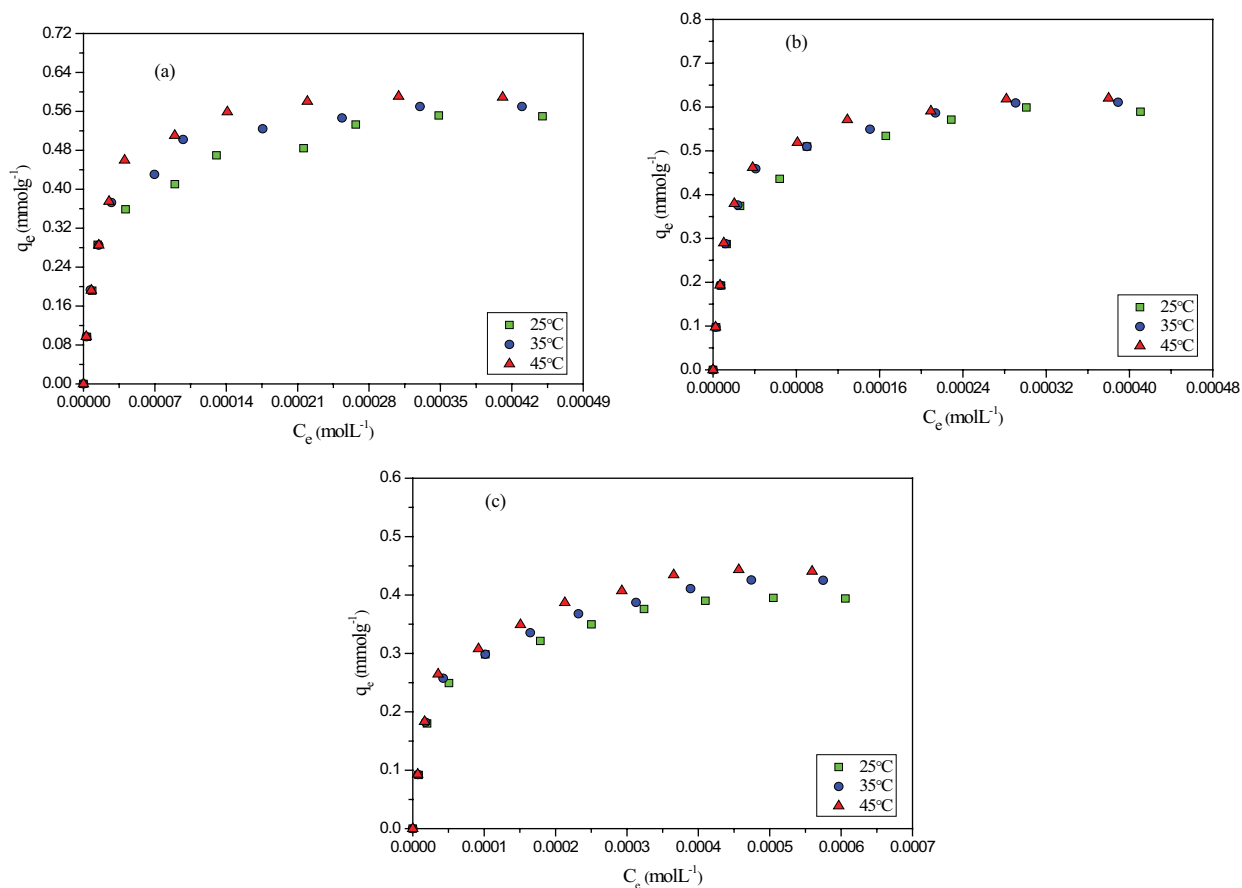


Fig. 3. Adsorption isotherms for the removal of (a) Basic red 2, (b) Basic blue 3 and (c) Ethyl orange on DKLAAC at different temperatures.

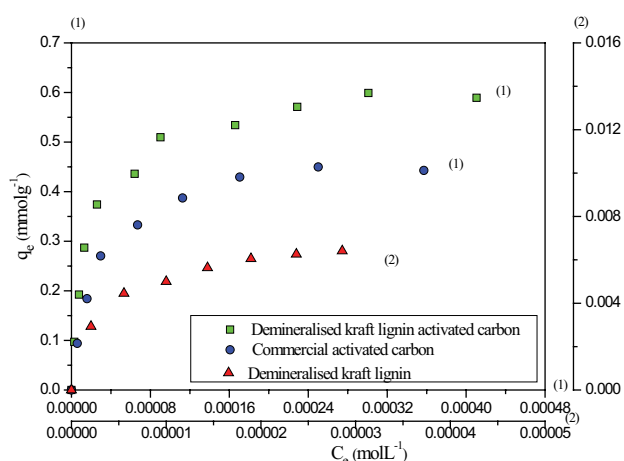


Fig. 4. Adsorption isotherms for the removal of Basic red 2 on DKLAAC, CAC and DKL at 25°C.

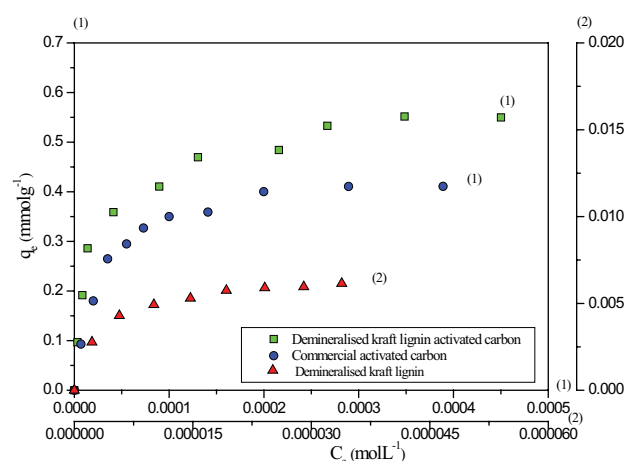


Fig. 5. Adsorption isotherms for the removal of Basic blue 3 on DKLAAC, CAC and DKL at 25°C.

values of studied dyes on DKLAAC were compared with other materials as available in the literature and are presented in Table 4. It can be observed from Table 4 that the amount of adsorption of these dyes on the DKLAAC is more efficient and as good as other adsorbents reported in literature.

The effect of solution temperature on the adsorptive removal of dyes with almost similar molecular weight but different in class and group functionality on DKLAAC was investigated in the temperature range between 25°C to 45°C and the adsorption isotherms are shown in Fig. 3. It is observed that the adsorption of Basic red 2, Basic blue 3

and Ethyl orange dyes onto DKLAAC increases from 0.599 to 0.620, 0.550 to 0.589 and 0.395 to 0.443 mmol g<sup>-1</sup>, respectively, which indicating the process to be endothermic in nature. It is noteworthy that the main reason for this trend is the mass diffusion of dyes molecules at the external boundary layer and in the inner pores of the adsorbent particle which increases with increase in temperature, owing to decrease in the viscosity of the adsorbate solution [28–32].

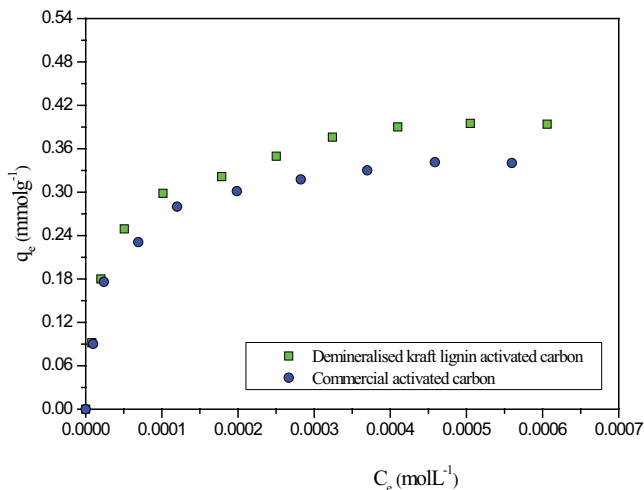


Fig. 6. Adsorption isotherms for the removal of Ethyl orange on DKLAAC and CAC at 2.

Table 4

Comparison of the adsorption capacities of the developed activated carbon for Basic red 2, Basic blue 3 and Ethyl orange with some other adsorbents reported previously

| S. No.       | Adsorbent   | Max. adsorbed amount (mg g <sup>-1</sup> ) | References |
|--------------|---|--|------------|
| Basic red 2  |   |  |            |
| 1.           | Phosphoric acid modified coconut coir             | 96.81                                      | [43]       |
| 2.           | Date pits   | 92   | [44]       |
| 3.           | Poly lignin nanoparticles glycol polyacrylic acid | 138.88                                     | [45]       |
| 4.           | Natural raw kaolinite                             | 16.23                                      | [46]       |
| 5.           | Avocado integuments                               | 15.6                                       | [47]       |
| 6.           | DKLAAC  | 210  | This work  |
| Basic blue 3 |   |  |            |
| 1.           | Macadamia seed husks                              | 1.4  | [48]       |
| 2.           | Ternary nanocomposite (Gum Arabic/PVA/Alginate)   | 200  | [49]       |
| 3.           | Pineapple plant stem                              | 58.983                                     | [50]       |
| 4.           | Durian peel                                       | 49.50                                      | [51]       |
| 5.           | Ethylenediamine modified rice hull                | 14.68                                      | [52]       |
| 6.           | DKLAAC  | 197  | This work  |
| Ethyl orange |   |  |            |
| 1.           | Carbon slurry                                     | 233  | [53]       |
| 2.           | ZnO hybrid chitosan                               | 0.014                                      | [54]       |
| 3.           | Carbon slurry                                     | 198  | [55]       |
| 4.           | DKLAAC  | 140  | This work  |

Furthermore, to analyse the adsorption mechanism of dyes on DKLAAC, Langmuir and Freundlich models were used and the results are shown in Table 3. The mathematical form of the Langmuir equation [33] is shown as:

$$\frac{1}{q_e} = \frac{1}{q_{\max}} + \frac{1}{q_{\max} b C_e} \quad (1)$$

where  $C_e$  is the concentration of dye in the solution at equilibrium,  $q_e$  is the adsorbed amount of dye at equilibrium,  $q_{\max}$  is the theoretical maximum adsorption capacity also known as Langmuir monolayer capacity and  $b$  is the adsorption equilibrium constant for Langmuir isotherm. The plot between  $1/q_e$  and  $1/C_e$  for the adsorption of Basic red 2, Basic blue 3 and Ethyl orange have been drawn and shown only for Basic red 2 in Fig. 7 (plots being same for Basic blue 3 and Ethyl orange hence not shown here). The calculated Langmuir parameters  $q_{\max}$  and  $b$  are given in Table 3. The Langmuir monolayer capacity ( $q_{\max}$ ) and adsorption equilibrium constant for Langmuir isotherm ( $b$ ) for Basic red 2, Basic blue 3 and Ethyl orange were found to be 0.569, 0.520 and 0.387 mmol g<sup>-1</sup> and  $7.14 \times 10^4$ ,  $6.93 \times 10^4$  and  $3.89 \times 10^4$  L mmol<sup>-1</sup>, respectively at 25°C. These results clearly state that the values are comparable to the experimental adsorption capacity ( $q_{\text{exp}}$ ) and shows maximum affinity for Basic red 2 and minimum for Ethyl orange. The values of  $q_{\max}$  as well as  $b$  increased on increasing the temperature indicating the endothermic nature of the process. The  $R_L$  values for the dyes were found to lie between

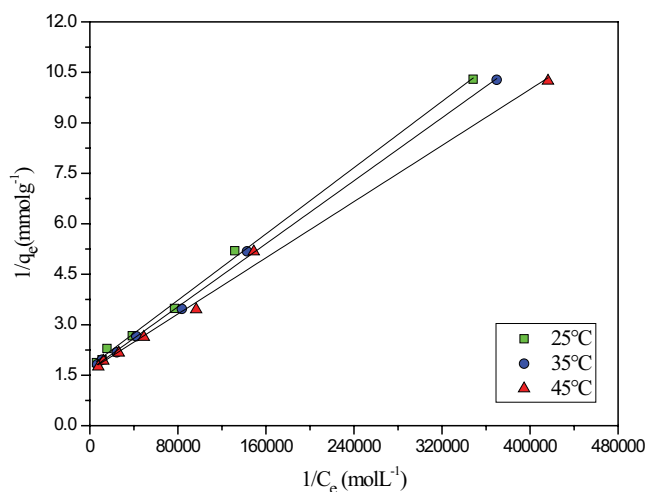


Fig. 7. Langmuir adsorption isotherms of Basic red 2 on DKLAAC at different temperatures.

0 and 1, which confirm the favorability of the adsorption isotherm [34].

Besides Langmuir isotherm, the adsorption data of the similar molecular weight dyes (acid/basic dyes) was also analysed by Freundlich model [35] shown as:

$$\log q_e = \log K_f + \log C_e \quad (2)$$

where  $q_e$  is the amount adsorbed at the equilibrium concentration,  $K_f$  is an indicator of adsorption capacity and  $n$  is heterogeneity factor. A plot between  $\log q_e$  vs.  $\log C_e$  was made and shown in Fig. 8 for the dye Basic red 2 (plots being same for Basic blue 3 and Ethyl orange are not shown here). The values of Freundlich constants ( $K_f$  and  $1/n$ ) were calculated from the intercept and slope, respectively and are presented in Table 3. The low correlation coefficient ( $R^2$ ) values obtained for Freundlich comparatively to the Langmuir isotherm model, further confirm that the process can be described well by the Langmuir model. Furthermore, the theoretical values of adsorption capacity observed by the Langmuir model were close to the experimental value, hence supporting our view that the Langmuir model fits well to the process.

The results show that the investigated dyes do not have a big difference in their adsorption values on DKLAAC. The reason could be that DKLAAC is neither too acidic nor too basic in nature. It has a pzc of 7.5 which makes it slightly amphoteric in nature, therefore, do not attract or repel the molecules due to its charge. However, it is worth noting that besides other factors hydrogen bonding and electrostatic interactions between dyes and oxygen-containing functional groups (Table 2) on carbons are also responsible for dye adsorption.

The difference observed in the adsorption values of dyes can be explained on the basis of two factors, firstly, the presence of acid/basic site concentration on carbons and secondly, the difference in the structure of dyes molecules. Basic dyes adsorbed more as compared to acidic dyes on DKLAAC owing to more acidic sites (Table 2). A similar

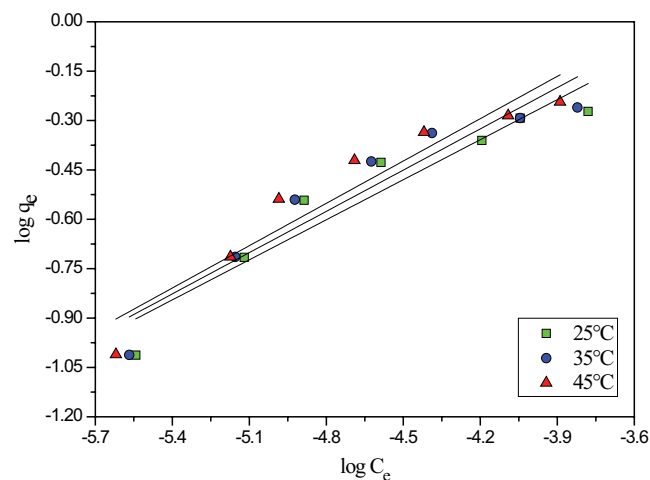


Fig. 8. Freundlich adsorption isotherms of Basic red 2 on DKLAAC at different temperatures.

trend was observed in the case of CAC since it also has more acidic sites ( $0.579 \text{ mmol g}^{-1}$ ) than basic sites ( $0.360 \text{ mmol g}^{-1}$ ) with a pzc (7.6) and functional groups as observed from FTIR (Table 2) similar to DKLAAC. Nevertheless, the three dyes (Basic red 2, Basic blue 3 and Ethyl orange) used in this study have almost the same molecular weight but differ in their chemical class and functional groups which also makes a difference in their adsorption behavior. Basic red 2 is a cationic dye of the azine group and its chemical structure is different from the two others. Basic red 2 showed better interaction with the DKLAAC as resonance is more in Basic red 2 due to the presence of an extra benzene ring [36]. Though, Basic blue 3 is also a cationic dye but belongs to oxazine class, showed slightly less adsorption capacity than Basic red 2 due to the lesser number of the benzene ring. However, the difference in the adsorption amount of Basic blue 3 and Basic red 2 is not too big which may be attributed to another factor, that is, hydrophobicity. Basic blue 3 has a chemical structure which is more hydrophobic due to the presence of four ethyl groups in the structure creating more affinity towards DKLAAC [37] whereas, Basic red 2 contains only two methyl group making it less hydrophobic. Ethyl orange which is an anionic azo dye had the least adsorption on DKLAAC owing to more hydrophilicity. Ethyl orange has a sulphonic group which enhances its hydrophilicity, moreover, it is reported that any dye which has less number of the ring [36] in their structure, also have less adsorption. Thus Ethyl orange having only two benzene rings is expected to have the least stabilization. This could be the main reason that Ethyl orange has the least adsorption among the dyes.

### 3.3. Thermodynamic studies

The thermodynamic parameters such as free energy change ( $\Delta G^\circ$ ), enthalpy change ( $\Delta H^\circ$ ) and entropy change ( $\Delta S^\circ$ ) have great importance in determining the feasibility, heat change and spontaneity of the adsorption process, respectively. These parameters were obtained utilising the equations:

$$\Delta G^\circ = -RT \ln(b) \quad (3)$$

$$\ln b = -\frac{\Delta H^\circ}{RT} + \frac{\Delta S^\circ}{R} \quad (4)$$

where  $T$  is the adsorption temperature,  $R$  is the gas constant ( $8.314 \text{ J mol}^{-1} \text{ K}^{-1}$ ) and  $b$  is the equilibrium constant for the adsorption process. A graph is plotted between  $\ln b$  vs.  $1/T$  (Van't Hoff plot) using Eq. (3) (Fig. 9) and from the slope and intercept of the plot, the values of change in enthalpy and entropy were obtained, respectively, and are presented in Table 5.

The values of  $\Delta G^\circ$ ,  $\Delta H^\circ$  and  $\Delta S^\circ$  for the dyes having similar molecular weight are presented in Table 5. Table 5 reveals that the negative values of  $\Delta G^\circ$  is indicative of the spontaneity and physisorptive nature of the adsorption process, whereas, the positive values of enthalpy change ( $\Delta H^\circ$ ) indicated that the process is endothermic in nature. Moreover,  $\Delta G^\circ$  values increases on increasing the temperature which supports the fact that the process is more spontaneous at higher temperatures. In addition the positive values of  $\Delta S^\circ$  is an indicator of the increased randomness/disorder on the solid/solution interface and affinity of the dyes for DKLAAC.

### 3.4. Kinetic studies

To investigate the mechanism and rate-controlling steps of adsorption processes like chemical reaction and mass transfer, kinetics of the process for the adsorption of the dyes having an almost similar molecular weight (Basic red 2, Basic blue 3 and Ethyl orange) has been carried out in time interval of 240 min. Different kinetic models such as pseudo-first-order, pseudo-second-order and intraparticle diffusion model are applied to test the experimental data [38].

Pseudo-first-order [39] (Eq. (5) and Fig. 10) and pseudo-second-order rate equation [40] (Eq. (6) and Fig. 11) are represented linearly as:

$$\log(q_e - q_t) = \log q_e - \frac{k_1}{2.303} t \quad (5)$$

$$\frac{t}{q_t} = \frac{1}{k_2 q_e^2} + \frac{1}{q_e} t \quad (6)$$

where  $q_e$  and  $q_t$  are the amount of dye adsorbed on DKLAAC at equilibrium and time  $t$ , respectively.  $k_1$  and  $k_2$  are the rate constants for pseudo-first and second-order-rate equation, respectively.

The values of  $q_e$ ,  $k_1$  and  $k_2$  are calculated from the slopes and intercepts of the respective plots and the values are provided in Table 6. Besides the theoretically calculated values, the correlation coefficients ( $R^2$ ) for both models were determined too and given in Table 6. Results revealed the better fitting of pseudo-second-order model over the pseudo-first-order rate equation due to the higher  $R^2$  values for the dyes, having similar molecular weight. Moreover, the theoretically calculated values ( $q_{e(\text{exp})}$ ) were found to be in close relation with the experimental values ( $q_{e(\text{cal})}$ ), which, further supports the better applicability of the pseudo-second-order model for the adsorption process. The root mean square error (RMSE) values were also evaluated to compare the prediction errors for the two models and were found to be in the range 0.002–0.004 for the pseudo-second-order model, whereas, for pseudo-first-order the values were found to be in the range 0.218–0.336. The low RMSE values for pseudo-second-order model further confirmed its applicability over the pseudo-first-order kinetic model.

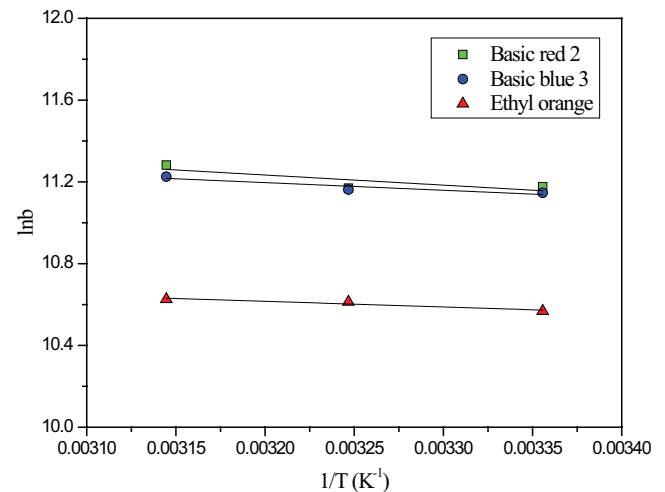


Fig. 9. Van't Hoff plots for the removal of Basic red 2, Basic blue 3 and Ethyl orange on DKLAAC.

Table 5  
Thermodynamic parameters for the removal of similar molecular weight acid/basic dyes on DKLAAC

| Dyes         | Temperature (°C) | $-\Delta G^\circ$ (kJ mol <sup>-1</sup> ) | $\Delta S^\circ$ (J mol <sup>-1</sup> K <sup>-1</sup> ) | $\Delta H^\circ$ (kJ mol <sup>-1</sup> ) |
|--------------|------------------|---|---|--|
| Basic red 2  | 25               | 27.7                                      | 106.9   | 4.11                                     |
|              | 35               | 28.6                                      |   |  |
|              | 45               | 29.8                                      |   |  |
| Basic blue 3 | 25               | 27.6                                      | 103.2   | 3.11                                     |
|              | 35               | 28.6                                      |   |  |
|              | 45               | 29.7                                      |   |  |
| Ethyl orange | 25               | 26.2                                      | 95.6  | 2.29                                     |
|              | 35               | 27.2                                      |   |  |
|              | 45               | 28.1                                      |   |  |



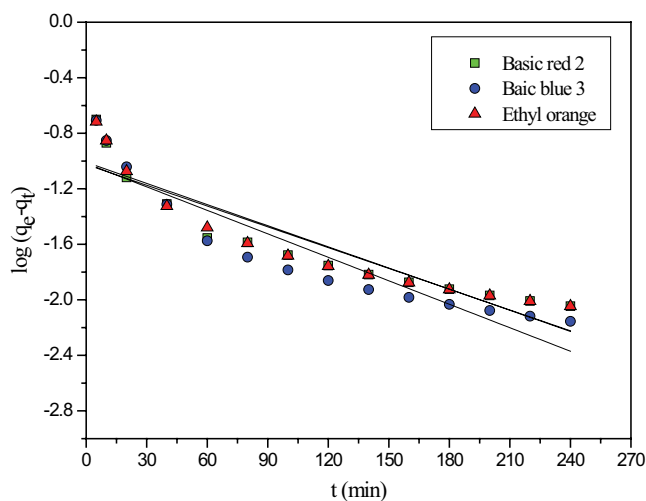


Fig. 10. Pseudo-first-order kinetic plot for the removal of Basic red 2, Basic blue 3 and Ethyl orange on DKLAAC (Initial concentration:  $5 \times 10^{-4}$  M and  $T: 25^\circ\text{C}$ ).

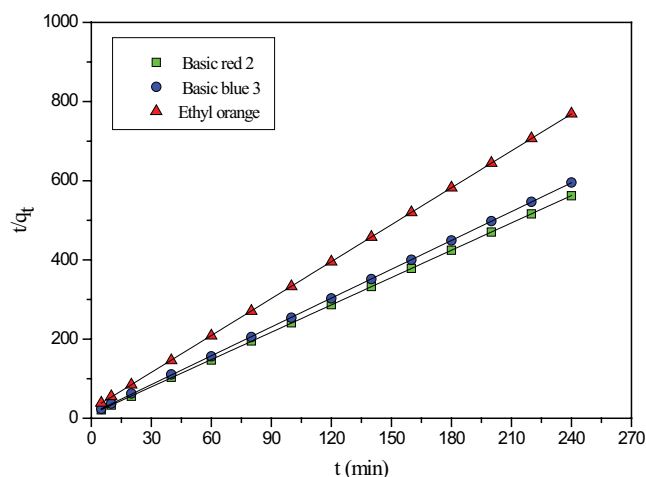


Fig. 11. Pseudo-second-order kinetic plot for the removal of Basic red 2, Basic blue 3 and Ethyl orange on DKLAAC (Initial concentration:  $5 \times 10^{-4}$  M and  $T: 25^\circ\text{C}$ ).

The two kinetic models can also be conveniently estimated via nonlinear regression method too using the original form of the equations given below:

$$q_t = q_e (1 - \exp^{-k_1 t}) \quad (7)$$

$$q_t = \frac{k_2 q_e^2 t}{1 + k_2 q_e t} \quad (8)$$

The high correlation coefficients ( $\sim 0.999$ ) and low RMSE (0.001–0.004) values obtained for the three dyes by non linear regression in case of the pseudo-second-order model as compared to the low correlation coefficients (0.977–0.987) and high RMSE (0.009–0.016) values obtained in case of pseudo-first-order model further confirmed that pseudo-second-order model fits better to our process.

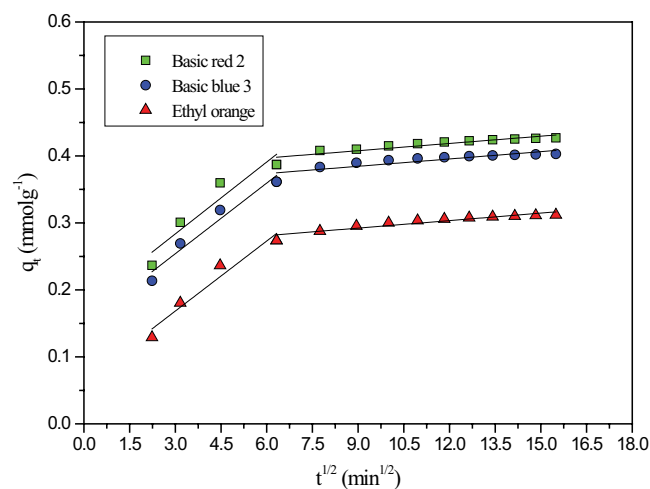


Fig. 12. Intraparticle diffusion kinetic plot for the removal of Basic red 2, Basic blue 3 and Ethyl orange on DKLAAC (Initial concentration:  $5 \times 10^{-4}$  M and  $T: 25^\circ\text{C}$ ).

*Intraparticle diffusion model:* Additionally, the intraparticle diffusion model by Weber and Morris [41] was also applied to the experimental kinetic data in order to investigate the rate-controlling step of the adsorption process of almost similar molecular weight dyes onto DKLAAC.

Weber–Morris plot can be used to determine the rate controlling step and the intraparticle diffusion rate constant was calculated utilising the equation:

$$q_t = k_{id} \cdot t^{1/2} + C \quad (9)$$

where  $C$  and  $k_{id}$  are the constant for the thickness of the boundary layer and intraparticle diffusion. Fig. 12 shows that the plots do not pass through origin although have some degree of linearity which means that more than one step controls the adsorption process [42]. Moreover, the plots reveal the existence of two linear sections which were assigned to the film diffusion (I–Stage) and intraparticle diffusion (II–Stage). The value of intraparticle rate constants  $k_{id}$  and  $C$  ( $k_{id1}$  and  $C_1$  for I–stage and  $k_{id2}$  and  $C_2$  for II–stage) were determined using these plots and presented in Table 6. The results from Table 6 indicated that intraparticle diffusion is not solely responsible for the rate-controlling step. Therefore it can be assumed that the adsorption of these dyes on DKLAAC is a complex process and can be controlled by both, surface sorption and intraparticle diffusion.

#### 4. Conclusions

In the present work, the role of similar molecular weight dyes (Basic red 2, Basic blue 3 and Ethyl orange) belonging to the different chemical classes on the adsorption process was studied. The amount of the adsorption of these dyes on the DKLAAC was found to be 0.599, 0.550 and 0.395  $\text{mmol g}^{-1}$  for Basic red 2, Basic blue 3 and Ethyl orange, respectively at  $25^\circ\text{C}$ . Basic red 2 showed maximum adsorption due to more hydrophobicity and resonance in its structure, on the other hand, Ethyl orange showed minimum

Table 6  
Kinetic parameters for the removal of similar molecular weight acid/basic dyes on DKLAAC

| Dyes         | Pseudo-first-order           |   |   | Pseudo-second-order        |       |   | Intraparticle diffusion                         |       |           |       |       |           |       |       |
|--------------|------------------------------|---|---|----------------------------|-------|---|---|-------|-----------|-------|-------|-----------|-------|-------|
|              | $C_0$ (mol L <sup>-1</sup> ) | $q_{e(\text{exp})}$ (mmol g <sup>-1</sup> ) | $q_{e(\text{cal})}$ (mmol g <sup>-1</sup> ) | $k_1$ (min <sup>-1</sup> ) | $R^2$ | $q_{e(\text{cal})}$ (mmol g <sup>-1</sup> ) | $k_2$ (g mmol <sup>-1</sup> min <sup>-1</sup> ) | $R^2$ | $K_{ad1}$ | $C_1$ | $R^2$ | $K_{ad2}$ | $C_2$ | $R^2$ |
| Basic red 2  | $5 \times 10^{-4}$           | 0.436                                       | 0.095                                       | $1.15 \times 10^{-2}$      | 0.855 | 0.435                                       | 0.518   | 0.999 | 0.036     | 0.176 | 0.902 | 0.0036    | 0.375 | 0.844 |
| Basic blue 3 | $5 \times 10^{-4}$           | 0.410                                       | 0.096                                       | $1.30 \times 10^{-2}$      | 0.859 | 0.412                                       | 0.484   | 0.999 | 0.035     | 0.149 | 0.955 | 0.0036    | 0.352 | 0.783 |
| Ethyl orange | $5 \times 10^{-4}$           | 0.321                                       | 0.098                                       | $1.17 \times 10^{-2}$      | 0.868 | 0.322                                       | 0.428   | 0.999 | 0.035     | 0.064 | 0.950 | 0.0037    | 0.259 | 0.885 |

adsorption value owing to more hydrophilicity and less number of benzene rings. The small positive values of  $\Delta H^\circ$  4.11, 3.11 and 2.29 kJ mol<sup>-1</sup> obtained for Basic red 2, Basic blue 3 and Ethyl orange, respectively indicate that the adsorption is physical in nature involving weak forces of attraction. The Langmuir adsorption model fitted well to the process and high correlation coefficient values (0.994–0.999) were obtained for the process as compared to Freundlich model (0.896–0.934). The pseudo-second-order model was found to fit well for the adsorption of all dyes studied on the DKLAAC.

### Acknowledgements

One of the authors (Monika Chaudhary INSPIRE Fellow code IF120368) is grateful to the DST (Department of Science and Technology), New Delhi, India for the award of a doctoral grant (No. DST/INSPIRE Fellowship/2012/346).

### References

- [1] H.K. Yağmur, İ. Kaya, Synthesis and characterization of magnetic ZnCl<sub>2</sub>-activated carbon produced from coconut shell for the adsorption of methylene blue, *J. Mol. Struct.*, 130071 (2021) 1–12.
- [2] Z. Li, H. Hanafy, L. Zhang, L. Sellaoui, M.S. Netto, M.L. Oliveira, M.K. Seliem, G.L. Dotto, A. Bonilla-Petriciolet, Q. Li, Adsorption of congo red and methylene blue dyes on an ashitaba waste and a walnut shell-based activated carbon from aqueous solutions: experiments, characterization and physical interpretations, *Chem. Eng. J.*, 388 (2020) 124263, doi: 10.1016/j.cej.2020.124263.
- [3] T.N.V. de Souza, S.M.L. de Carvalho, M.G.A. Vieira, M.G.C. da Silva, D.d.S.B. Brasil, Adsorption of basic dyes onto activated carbon: experimental and theoretical investigation of chemical reactivity of basic dyes using DFT-based descriptors, *Appl. Surf. Sci.*, 448 (2018) 662–670.
- [4] A. Jain, V. Gupta, A. Bhatnagar, Suhas, A comparative study of adsorbents prepared from industrial wastes for removal of dyes, *Sep. Sci. Technol.*, 38 (2003) 463–481.
- [5] A. Kouhpayeh, M. Moazzen, G.R. Jahed Khaniki, S. Dobaradaran, N. Shariatifar, M. Ahmadloo, A. Azari, S. Nazmara, A. Kiani, M. Salari, Extraction and determination of phthalate esters (PAEs) in Doogh, *J. Maz. Univ. Med. Sci.*, 26 (2017) 257–267.
- [6] J. Rahmani, A. Miri, A. Mohseni-Bandpei, Y. Fakhri, G. Bjorklund, H. Keramati, B. Moradi, N. Amanidaz, N. Shariatifar, A.M. Khaneghah, Contamination and prevalence of histamine in canned tuna from Iran: a systematic review, meta-analysis, and health risk assessment, *J. Food Prot.*, 81 (2018) 2019–2027.
- [7] S. Sharifi, R. Nabizadeh, B. Akbarpour, A. Azari, H.R. Ghaffari, S. Nazmara, B. Mahmoudi, L. Shiri, M. Yousefi, Modeling and optimizing parameters affecting hexavalent chromium adsorption from aqueous solutions using Ti-XAD7 nanocomposite: RSM-CCD approach, kinetic, and isotherm studies, *J. Environ. Health Sci. Eng.*, 17 (2019) 873–888.
- [8] S. Nabizadeh, N. Shariatifar, E. Shokoohi, S. Shoeibi, M. Gavahian, Y. Fakhri, A. Azari, A. Mousavi Khaneghah, Prevalence and probabilistic health risk assessment of aflatoxins B1, B2, G1, and G2 in Iranian edible oils, *Environ. Sci. Pollut. Res.*, 25 (2018) 35562–35570.
- [9] A. Azari, M. Salari, M.H. Dehghani, M. Alimohammadi, H. Ghaffari, K. Sharafi, N. Shariatifar, M. Baziar, Efficiency of magnetized graphene oxide nanoparticles in removal of 2,4-dichlorophenol from aqueous solution, *J. Maz. Univ. Med. Sci.*, 26 (2017) 265–281.
- [10] D.J. Naghan, A. Azari, N. Mirzaei, A. Velayati, F.A. Tapouk, S. Adabi, M. Pirsaeheb, K. Sharafi, Parameters effecting on photocatalytic degradation of the phenol from aqueous

- solutions in the presence of ZnO nanocatalyst under irradiation of UV-C light, *Bulg. Chem. Commun.*, 47 (2015) 14–18.
- [11] A. Azari, A.-A. Babaie, R. Rezaei-Kalantary, A. Esrafil, M. Moazzen, B. Kakavandi, Nitrate removal from aqueous solution by carbon nanotubes magnetized with nano zero-valent iron, *J. Maz. Univ. Med. Sci.*, 23 (2014) 15–27.
- [12] M. Heydari Moghaddam, R. Nabizadeh, M.H. Dehghani, B. Akbarpour, A. Azari, M. Yousefi, Performance investigation of Zeolitic Imidazolate Framework-8 (ZIF-8) in the removal of trichloroethylene from aqueous solutions, *Microchem. J.*, 150 (2019) 104185, 1–9.
- [13] M.Y. Badi, A. Azari, A. Esrafil, E. Ahmadi, M. Gholami, Performance evaluation of magnetized multiwall carbon nanotubes by iron oxide nanoparticles in removing fluoride from aqueous solution, *J. Maz. Univ. Med. Sci.*, 25 (2015) 128–142.
- [14] E. Ahmadi, B. Kakavandi, A. Azari, H. Izanloo, H. Gharibi, A.H. Mahvi, A. Javid, S.Y. Hashemi, The performance of mesoporous magnetite zeolite nanocomposite in removing dimethyl phthalate from aquatic environments, *Desal. Water Treat.*, 57 (2016) 27768–27782.
- [15] V.K. Gupta, Suhas, Application of low-cost adsorbents for dye removal – a review, *J. Environ. Manage.*, 90 (2009) 2313–2342.
- [16] F. Deniz, S. Karaman, Removal of Basic Red 46 dye from aqueous solution by pine tree leaves, *Chem. Eng. J.*, 170 (2011) 67–74.
- [17] P.F. Gordon, P. Gregory, *Organic Chemistry in Colour*, Springer, Berlin Heidelberg, 2012.
- [18] K. Venkataraman, M.E. Fieser, L.F. Fieser, *The Chemistry of Synthetic Dyes*, Vol. 2, Academic Press Inc., New York, 2013.
- [19] P. Bamfield, M.G. Hutchings, *Chromic Phenomena: Technological Applications of Colour Chemistry*, Royal Society of Chemistry, 2010.
- [20] K. Hunger, *Industrial Dyes: Chemistry, Properties, Application*, Wiley-VCH, 2003.
- [21] Suhas, P.J.M. Carrott, M.M.L.R. Carrott, R. Singh, L.P. Singh, M. Chaudhary, An innovative approach to develop microporous activated carbons in oxidising atmosphere, *J. Cleaner Prod.*, 156 (2017) 549–555.
- [22] J.M. Valente Nabais, P.J.M. Carrott, Chemical characterization of activated carbon fibers and activated carbons, *J. Chem. Educ.*, 83 (2006) 436–438.
- [23] M. Chaudhary, Suhas, R. Singh, I. Tyagi, J. Ahmed, S. Chaudhary, S. Kushwaha, Microporous activated carbon as adsorbent for the removal of noxious anthraquinone acid dyes: role of adsorbate functionalization, *J. Environ. Chem. Eng.*, 9 (2021) 106308, 1–12.
- [24] A.B. Albadarin, M.N. Collins, M. Naushad, S. Shirazian, G. Walker, C. Mangwandi, Activated lignin-chitosan extruded blends for efficient adsorption of methylene blue, *Chem. Eng. J.*, 307 (2017) 264–272.
- [25] C. Duran, D. Ozdes, A. Gundogdu, H.B. Senturk, Kinetics and isotherm analysis of basic dyes adsorption onto almond shell (*Prunus dulcis*) as a low cost adsorbent, *J. Chem. Eng. Data*, 56 (2011) 2136–2147.
- [26] A. Mary Ealias, M.P. Saravanakumar, A critical review on ultrasonic-assisted dye adsorption: mass transfer, half-life and half-capacity concentration approach with future industrial perspectives, *Crit. Rev. Environ. Sci. Technol.*, 49 (2019) 1959–2015.
- [27] R. Lafi, I. Montasser, A. Hafiane, Adsorption of congo red dye from aqueous solutions by prepared activated carbon with oxygen-containing functional groups and its regeneration, *Adsorpt. Sci. Technol.*, 37 (2019) 160–181.
- [28] L.M. Cotoruelo, M.D. Marqués, F.J. Díaz, J. Rodríguez-Mirasol, J.J. Rodríguez, T. Cordero, Lignin-based activated carbons as adsorbents for crystal violet removal from aqueous solutions, *Environ. Prog. Sustainable Energy*, 31 (2012) 386–396.
- [29] O. Sözüdoğru, B.A. Fil, R. Boncukcuoğlu, E. Aladağ, S. Kul, Adsorptive removal of cationic (BY2) dye from aqueous solutions onto Turkish clay: isotherm, kinetic, and thermodynamic analysis, *Part. Sci. Technol.*, 34 (2016) 103–111.
- [30] M. Yu, Y. Han, J. Li, L. Wang, CO<sub>2</sub>-activated porous carbon derived from cattail biomass for removal of malachite green dye and application as supercapacitors, *Chem. Eng. J.*, 317 (2017) 493–502.
- [31] X. Sun, P. Cheng, H. Wang, H. Xu, L. Dang, Z. Liu, Z. Lei, Activation of graphene aerogel with phosphoric acid for enhanced electrocapacitive performance, *Carbon*, 92 (2015) 1–10.
- [32] S. Rani, K. Sumanjit, R. Mahajan, Comparative study of surface modified carbonized *Eichhornia crassipes* for adsorption of dye safranin, *Sep. Sci. Technol.*, 50 (2015) 2436–2447.
- [33] I. Langmuir, The adsorption of gases on plane surfaces of glass, mica and platinum, *J. Am. Chem. Soc.*, 40 (1918) 1361–1403.
- [34] T.W. Weber, R.K. Chakravorti, Pore and solid diffusion models for fixed-bed adsorbents, *AIChE J.*, 20 (1974) 228–238.
- [35] H. Freundlich, Over the adsorption in solution, *J. Phys. Chem.*, 57 (1906) 1100–1107.
- [36] T. Wu, X. Cai, S. Tan, H. Li, J. Liu, W. Yang, Adsorption characteristics of acrylonitrile, p-toluenesulfonic acid, 1-naphthalenesulfonic acid and methyl blue on graphene in aqueous solutions, *Chem. Eng. J.*, 173 (2011) 144–149.
- [37] W.J. Weber, *Physicochemical Processes for Water Quality Control*, Wiley-Interscience, 1972.
- [38] F.-C. Wu, R.-L. Tseng, R.-S. Juang, Kinetic modeling of liquid-phase adsorption of reactive dyes and metal ions on chitosan, *Water Res.*, 35 (2001) 613–618.
- [39] S. Lagergren, About the theory of so-called adsorption of soluble substances, *Kungl. Svenska Vetenskapsakad. Handl.*, 24 (1898) 1–39.
- [40] Y.-S. Ho, G. McKay, Sorption of dye from aqueous solution by peat, *Chem. Eng. J.*, 70 (1998) 115–124.
- [41] W. Weber, J. Morris, *Advances in Water Pollution Research, Proceedings of the First International Conference on Water Pollution Research*, Pergamon Press Oxford, 1962, p. 231.
- [42] I. Kilic, E. Apaydin-Varol, A.E. Pütün, Adsorptive removal of phenol from aqueous solutions on activated carbon prepared from tobacco residues: equilibrium, kinetics and thermodynamics, *J. Hazard. Mater.*, 189 (2011) 397–403.
- [43] I. Ghosh, S. Kar, T. Chatterjee, N. Bar, S.K. Das, Adsorptive removal of Safranin-O dye from aqueous medium using coconut coir and its acid-treated forms: adsorption study, scale-up design, MPR and GA-ANN modeling, *Sustain. Chem. Pharm.*, 19 (2021) 100374, 1–23.
- [44] M. Wakkal, B. Khiari, F. Zagrouba, Basic red 2 and methyl violet adsorption by date pits: adsorbent characterization, optimization by RSM and CCD, equilibrium and kinetic studies, *Environ. Sci. Pollut. Res.*, 26 (2019) 18942–18960.
- [45] J. Azimvand, K. Didehban, S. Mirshokraie, Safranin-O removal from aqueous solutions using lignin nanoparticle-g-polyacrylic acid adsorbent: synthesis, properties, and application, *Adsorpt. Sci. Technol.*, 36 (2018) 1422–1440.
- [46] K.O. Adebowale, B.I. Olu-Owolabi, E.C. Chigbundu, Removal of safranin-O from aqueous solution by adsorption onto kaolinite clay, *J. Encapsulation Adsorpt. Sci.*, 4 (2014) 89–104.
- [47] F. Marahel, M.A. Khan, E. Marahel, I. Bayesti, S. Hosseini, Kinetics, thermodynamics, and isotherm studies for the adsorption of BR2 dye onto avocado integument, *Desal. Water Treat.*, 53 (2015) 826–835.
- [48] M.F. Mutunga, W.C. Wanyonyi, G. Ongera, Utilization of Macadamia seed husks as a low-cost sorbent for removing cationic dye (Basic blue 3 dye) from aqueous solution, *Environ. Chem. Ecotoxicol.*, 2 (2020) 194–200.
- [49] S. Karakuş, S. Şişmanoğlu, G. Akdut, Ö. Ür, E. Tan, T. Şişmanoğlu, A. Kilislioglu, Removal of Basic blue 3 from the aqueous solution with ternary polymer nanocomposite: swelling, kinetics, isotherms and error function, *J. Chem. Soc. Pak.*, 39 (2017) 17–25.
- [50] S.-L. Chan, Y.P. Tan, A.H. Abdullah, S.-T. Ong, Equilibrium, kinetic and thermodynamic studies of a new potential biosorbent for the removal of Basic blue 3 and Congo Red dyes: pineapple (*Ananas comosus*) plant stem, *J. Taiwan Inst. Chem. Eng.*, 61 (2016) 306–315.

- [51] S.-T. Ong, S.-Y. Tan, E.-C. Khoo, S.-L. Lee, S.-T. Ha, Equilibrium studies for Basic blue 3 adsorption onto durian peel (*Durio zibethinus Murray*), *Desal. Water Treat.*, 45 (2012) 161–169.
- [52] S.T. Ong, C.K. Lee, Z. Zainal, Removal of basic and reactive dyes using ethylenediamine modified rice hull, *Bioresour. Technol.*, 98 (2007) 2792–2799.
- [53] V. Gupta, Suhas, I. Tyagi, S. Agarwal, R. Singh, M. Chaudhary, A. Harit, S. Kushwaha, Column operation studies for the removal of dyes and phenols using a low cost adsorbent, *Global J. Environ. Sci. Manage.*, 2 (2016) 1–10.
- [54] N. Ngadi, M.A. Mahmud, M. Jusoh, R. Abd Rahman, H. Alias, Removal of Ethyl orange dye using hybrid chitosan and zinc oxide, *Jurnal Teknologi*, 67 (2014) 47–52.
- [55] A.K. Jain, V.K. Gupta, A. Bhatnagar, Suhas, Utilization of industrial waste products as adsorbents for the removal of dyes, *J. Hazard. Mater.*, 101 (2003) 31–42.